These results demonstrate the ability of present-day ultrashort-laser–driven x-ray sources to study transiently generated extreme states of matter. Although further studies of important outstanding problems related to the structure of superheated solids and transient liquid phases (*1*, *2*) are natural extensions of this work, foreseeable improvements already in development in tabletop laser-driven plasma sources should expand the scope of ultrafast x-ray diffraction to the dynamic study of many other ultrafast processes in physics, chemistry, and biology, including the ultrafast atomic and molecular dynamics by which other solid-state processes and chemical and biochemical reactions take place.

**References and Notes**


1. N. Bloembergen, *Nature* **356**, 110 (1992); D. H. Reitze, H. Ahn, M. C. Downer, *Phys. Rev. B* **45**, 2677 (1992).
2. G. Galli, R. M. Martin, R. Car, M. Parrinello, *Science* **250**, 1547 (1990).
3. R. W. Schoenlein *et al.*, *Science* **274**, 236 (1996).
4. C. Rischel *et al.*, *Nature* **390**, 490 (1997).
5. M. M. Murnane, H. C. Kapteyn, M. D. Rosen, R. W. Falcone, *Science* **251**, 531 (1991).
6. J. Larsson *et al.*, *Appl. Phys. A* **66**, 587 (1998).
7. C. Rose-Petruck *et al.*, *Nature* **398**, 310 (1999).
8. A. H. Chin *et al.*, in *Ultrafast Phenomena XI*, T. Elsaesser, J. G. Fujimoto, D. A. Wiersma, W. Zinth, Eds. (Springer, Berlin, 1998), pp. 401–403.
9. A. Cavalleri *et al.*, Quantum Electronics and Laser Science Conference (QELS) '99, postdeadline session QPD8, Baltimore, MD (1999); A. Rousse, Conference on Lasers and Electro-optics (CLEO) '99, session JWC1, Baltimore, MD (1999); A. M. Lindenberg *et al.*, QELS '99, session QThJ4, Baltimore, MD (1999).
10. J. A. Van Vechten, R. Tsu, F. W. Saris, *Phys. Lett. A* **74A**, 422 (1979).
11. N. Fabricius, P. Hermes, D. von der Linde, A. Pospieszczyk, B. Stritzker, *Solid State Commun*. **58**, 239 (1986).
12. M. C. Downer and C. V. Shank, *Phys. Rev. Lett*. **56**, 761 (1986).
13. F. Spaepen and D. Turnbull, in *Laser Annealing of Semiconductors*, J. M. Poate and J. W. Mayer, Eds. (Academic Press, London, 1982), pp. 15–42.
14. R. F. Wood and C. W. White, *Pulsed Laser Processing of Semiconductors, Semiconductors and Semimetals* (Academic Press, Orlando, FL, 1984), vol. 23.
15. C. V. Shank, R. Yen, C. Hirlimann, *Phys. Rev. Lett*. **50**, 454 (1983); *Phys. Rev. Lett*. **51**, 900 (1983).
16. H. W. K. Tom, G. D. Aumiller, C. H. Brito-Cruz, *Phys. Rev. Lett*. **60**, 1438 (1988).
17. P. Saeta, J. K. Wang, Y. Siegal, N. Bloembergen, E. Mazur, *Phys. Rev. Lett*. **67**, 1023 (1991).
18. K. Sokolowski-Tinten, J. Bialkowski, D. von der Linde, *Phys. Rev. B* **51**, 14186 (1995).
19. H. Li, J. P. Callan, E. N. Glezer, E. Mazur, *Phys. Rev. Lett*. **80**, 185 (1998).
20. K. Sokolowski-Tinten, J. Bialkowski, M. Boing, A. Cavalleri, D. von der Linde, *Phys. Rev. B* **58**, R11805 (1998).
21. M. Horn-von Hoegen, M. Copel, J. C. Tsang, M. C. Reuter, R. M. Tromp, *Phys. Rev. B* **50**, 10811 (1994); M. Horn-von Hoegen, *Appl. Phys. A* **A59**, 503 (1994).
22. Our experimental setup, discussed previously in (*7*), consisted of a visible-pump x-ray probe apparatus, with which the 8-keV (1.54 Å) bursts of Cu-$K_\alpha$ line radiation were generated by focusing 80-mJ, 30-fs pulses from a multiterawatt laser (*28*) at relativistic intensities onto a moving copper wire. X-ray pulses emitted from the plasma point source were diffracted by a photoexcited (111)-Ge crystal in a symmetric Bragg configuration and were recorded with a photon-counting area detector. The optical pump pulse, split off from the x-ray–generating laser pulse, was independently adjustable in both energy and pulsewidth. Focused onto the sample with a cylindrical lens, the pump pulse illuminated a ~0.4 mm by 2 mm region of the crystal that was sufficiently larger in the angular (that is, horizontal) direction than the area probed by the x-rays. Using a silicon wafer target, the pump fluence was first empirically set to the melting fluence of silicon, as evidenced by post-irradiation examination (*29*), and then increased to 0.5 J/cm$^2$, which is more than twice the known melting threshold for Ge. To avoid plasma formation in air or at the surface of the sample, the pump-pulse duration was increased to 100 fs, where no effects of plasma formation were observed.
23. B. C. Larson, C. W. White, T. S. Noggle, D. Mills, *Phys. Rev. Lett*. **48**, 337 (1982).
24. K. Sokolowski-Tinten *et al.*, *Phys. Rev. Lett*. **81**, 224 (1998).
25. Postmortem examination with interference microscopy did indicate crater formation, with an estimated upper limit of a crater depth of 15 nm. As expected from optical measurements (*24*), the crater diameter was significantly smaller than the transiently disordered area. Amorphous rings (*29*), which were observed with bulk silicon samples used to set the incident fluence, were not visible on the Ge films.
26. D. von der Linde, in *Resonances*, M. D. Levenson, E. Mazur, P. S. Pershan, Y. R. Shen, Eds. (World Scientific, Singapore, 1990).
27. P. Stampfli and K. H. Bennemann, *Phys. Rev. B* **49**, 7299 (1994); *Phys. Rev. B* **46**, 10686 (1992); *Phys. Rev. B* **42**, 7163 (1990).
28. C. P. J. Barty *et al.*, *Opt. Lett*. **21**, 668 (1996).
29. J. M. Liu, *Opt. Lett*. **7**, 196 (1982).


30. K.S.T. gratefully acknowledges financial support by the Deutsche Forschungsgemeinschaft.

15 July 1999; accepted 23 September 1999


# Cretaceous Sauropods from the Sahara and the Uneven Rate of Skeletal Evolution Among Dinosaurs


**Paul C. Sereno,[1]* Allison L. Beck,[1] Didier B. Dutheil,[2] Hans C. E. Larsson,[1] Gabrielle H. Lyon,[3] Bourahima Moussa,[4] Rudyard W. Sadleir,[5] Christian A. Sidor,[1] David J. Varricchio,[6] Gregory P. Wilson,[7] Jeffrey A. Wilson[8]**



**Lower Cretaceous fossils from central Niger document the succession of sauropod dinosaurs on Africa as it drifted into geographic isolation. A new broad-toothed genus of Neocomian age (~135 million years ago) shows few of the specializations of other Cretaceous sauropods. A new small-bodied sauropod of Aptian-Albian age (~110 million years ago), in contrast, reveals the highly modified cranial form of rebbachisaurid diplodocoids. Rates of skeletal change in sauropods and other major groups of dinosaurs are estimated quantitatively and shown to be highly variable.**


Breakup of the supercontinent Pangaea resulted in the differentiation of dinosaurian faunas that had been relatively uniform until the close of the Jurassic (*1*). Recent fossil discoveries on southern continents highlight the complexity of Cretaceous dinosaurian faunas (*2*–*4*). We report here on two new sauropod dinosaurs from central Niger that document the succession of these gigantic herbivores on northern Africa during the Early Cretaceous.

The fossils were discovered at several localities in the Neocomian [~140 to 130 million years ago (Ma)] Tiourarén Formation and in Aptian-Albian (~115 to 105 Ma) horizons of the Tegama Group in the Gadoufaoua region (Fig. 1).

The sauropod from the Tiourarén Formation, *Jobaria tiguidensis* gen. nov. sp. nov. (*5*), is the most abundant terrestrial vertebrate in the formation; no remains of any other large-bodied herbivore were recovered. The formation consists predominantly of clay-rich overbank deposits, which in one locality have entombed several partial skeletons of different sizes (*6*) (Fako; Fig. 1A, locality 3). Associated dinosaurs include the theropod *Afrovenator* (*3*) and two smaller bodied predators of uncertain affinities.

The skull (Fig. 2, A and B) is proportionately smaller and lighter in construction than that in *Camarasaurus*. The total length of an


[1]Department of Organismal Biology and Anatomy, University of Chicago, 1027 East 57 Street, Chicago, IL 60637, USA. [2]Laboratoire de Paléontologie–EPHE–Muséum National d'Histoire Naturelle, 8 rue du Buffon, 75005 Paris, France. [3]Project Exploration, 5521 South Blackstone Avenue, Chicago, IL 60637, USA. [4]Centre des Sciences de la Terre, Centre National de Recherche Scientifique, 6 Boulevard Gabriel, 2100 Dijon, France. [5]Department of Earth and Environmental Sciences, University of Illinois at Chicago, 845 West Taylor Street, Chicago, IL 60607, USA. [6]Museum of the Rockies, Montana State University, Bozeman, MT 59717, USA. [7]University of California, Museum of Paleontology, 1101 Valley Life Sciences Building, Berkeley, CA 94720, USA. [8]Museum of Paleontology, University of Michigan, 1109 Geddes Road, Ann Arbor, MI 48109, USA.

*To whom correspondence should be addressed. Successive authors are listed alphabetically.

adult skull of *Jobaria*, for example, is comparable to that of a subadult *Camarasaurus*, which has substantially shorter limb bones (Table 1). The external naris is particularly large, and the snout is abbreviate anteriorly (Fig. 2, A and B), unlike macronarians such as *Brachiosaurus*. There are at least 20 teeth in the upper and lower jaws, and the spatulate crowns have a variable number of marginal denticles (*3*).

*Jobaria* has a relatively short neck composed of only 12 cervical vertebrae. The centra are only moderately elongate and show a distinct elevation of the anterior face (Fig. 3, A and B). One articulated neck was preserved in a fully dorsiflexed, C-shaped posture, suggesting that the cervical column had considerably more latitude in the sagittal plane than suggested recently for some other sauropods (*7*). Pleurocoels are divided in the cervical vertebrae but extend posteriorly only as far as the anterior dorsal vertebrae. All neural spines are simple (undivided) (Fig. 3, B and C), and all caudal centra are amphiplatyan (Fig. 3D). The first chevron has a unique inverted U shape. Middle chevrons are distinguished by a ridge crossing the blade; more distal chevrons become anteroposteriorly elongate (Fig. 3, G to I). Clavicles and gastralia, rarely preserved in sauropods (*8*), are present (Fig. 3, A and E). The proportions of the limbs are primitive; the forelimb is not as elongate relative to the hind limb as in *Brachiosaurus*, and the manus (relative to the forearm) is not as elongate as in *Camarasaurus* or other macronarians (*9*) (Table 1; metacarpal II/radius ratio $< 0.40$).

Despite its Cretaceous age, *Jobaria* is strikingly primitive. Primitive features include the abbreviate snout, terminally positioned nares, low number of cervical vertebrae, simple neural spines, and many other features and suggest that *Jobaria* lies outside the neosauropod radiation, which encompasses all other known Cretaceous sauropods (diplodocoids, *Camarasaurus*, brachiosaurids, and titanosaurs) (Fig. 4A) (*10*). *Jobaria* represents an unknown lineage of broad-toothed sauropods that had diverged by the Middle Jurassic some 30 to 40 million years earlier. During this substantial interval, relatively few skeletal changes accrued, as shown by the small number of diagnostic features for the species (*5*, *10*).

The sauropod from the Tegama Group, *Nigersaurus taqueti* gen. nov. sp. nov. (*11*), is a new basal diplodocoid represented by several partial skeletons. *Nigersaurus* is one of the most common vertebrates in the Gadoufaoua exposures. It is also one of the smallest sauropods on record, reaching a maximum body length of about 15 m. The fossiliferous exposures of the Tegama Group in the Gadoufaoua region consist almost entirely of cross-bedded fluvial

**Table 1.** Length measurements (centimeters) and ratios in *Jobaria tiguidensis*, *Shunosaurus lii* (*35*), and *Camarasaurus grandis* (*36*). All measurements for *J. tiguidensis* are from MNN TIG3 except metatarsal III, which comes from an equal-sized individual (MNN TIG4). Length estimates for the radius and manual ungual I in *Camarasaurus* are based on *C. lentus* (*37*). Abbreviations: f, femur; h, humerus; mcII, metacarpal II; mtIII, metatarsal III; r, radius; and t, tibia. Parentheses indicate estimated measurements.

| Measurement | *Shunosaurus* | *Jobaria* | *Camarasaurus* |
|---|---|---|---|
| Skull | 37 | (73) | (75) |
| Cervical number, total length | 13, (130) | 12, (403) | 12, (299) |
| Humerus | 67 | 136 | 113 |
| Radius | 48 | 104 | (75) |
| Metacarpal II | 16 | 39 | 32 |
| Manual I ungual | 23 | 18 | (15) |
| Femur | 120 | 180 | 149 |
| Tibia | 68 | 108 | 93 |
| Metatarsal III | 18 | 30 | 22 |
| r/h | 0.72 | 0.77 | 0.66 |
| mcII/r | 0.33 | 0.38 | 0.43 |
| h/f | 0.56 | 0.76 | 0.76 |
| t/f | 0.57 | 0.60 | 0.62 |
| mtIII/t | 0.27 | 0.28 | 0.24 |

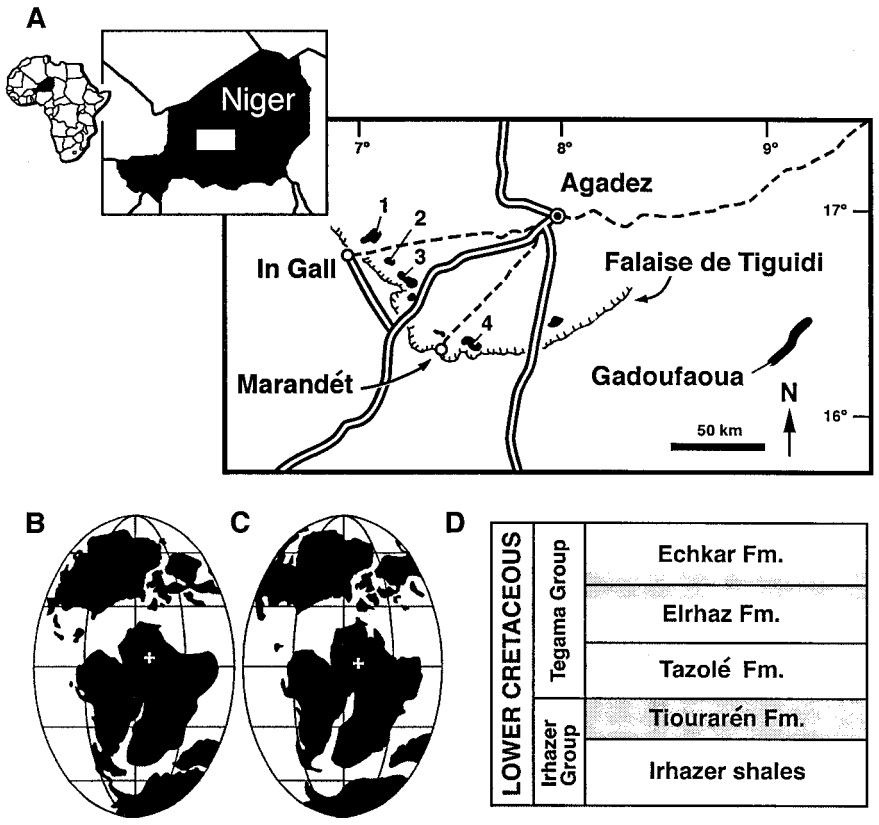


**Fig. 1.** Early Cretaceous paleogeography and principal fossiliferous exposures in central Niger. (**A**) Maps showing Niger and the location of the fossiliferous exposures in the Tiourarén Formation (localities: 1, Tiourarén and In Kaf; 2, Tamerát; 3, Fako and In Abaka; and 4, Tawachi) and middle horizons of the Tegama Group (Gadoufaoua); latitude in degrees north, longitude in degrees east. (**B**) Hauterivian-Barremian (~130 Ma) and (**C**) Albian (~110 Ma) Early Cretaceous paleogeographic maps (Molleweide projection) with latitude and longitude lines spaced at 30° intervals (longitude greater than 60° not shown) (*34*). White crosses indicate the fossiliferous exposures discussed in this report. (**D**) Geologic subdivision of Lower Cretaceous rocks in central Niger with fossiliferous levels in gray (*12*). Fm, formation.

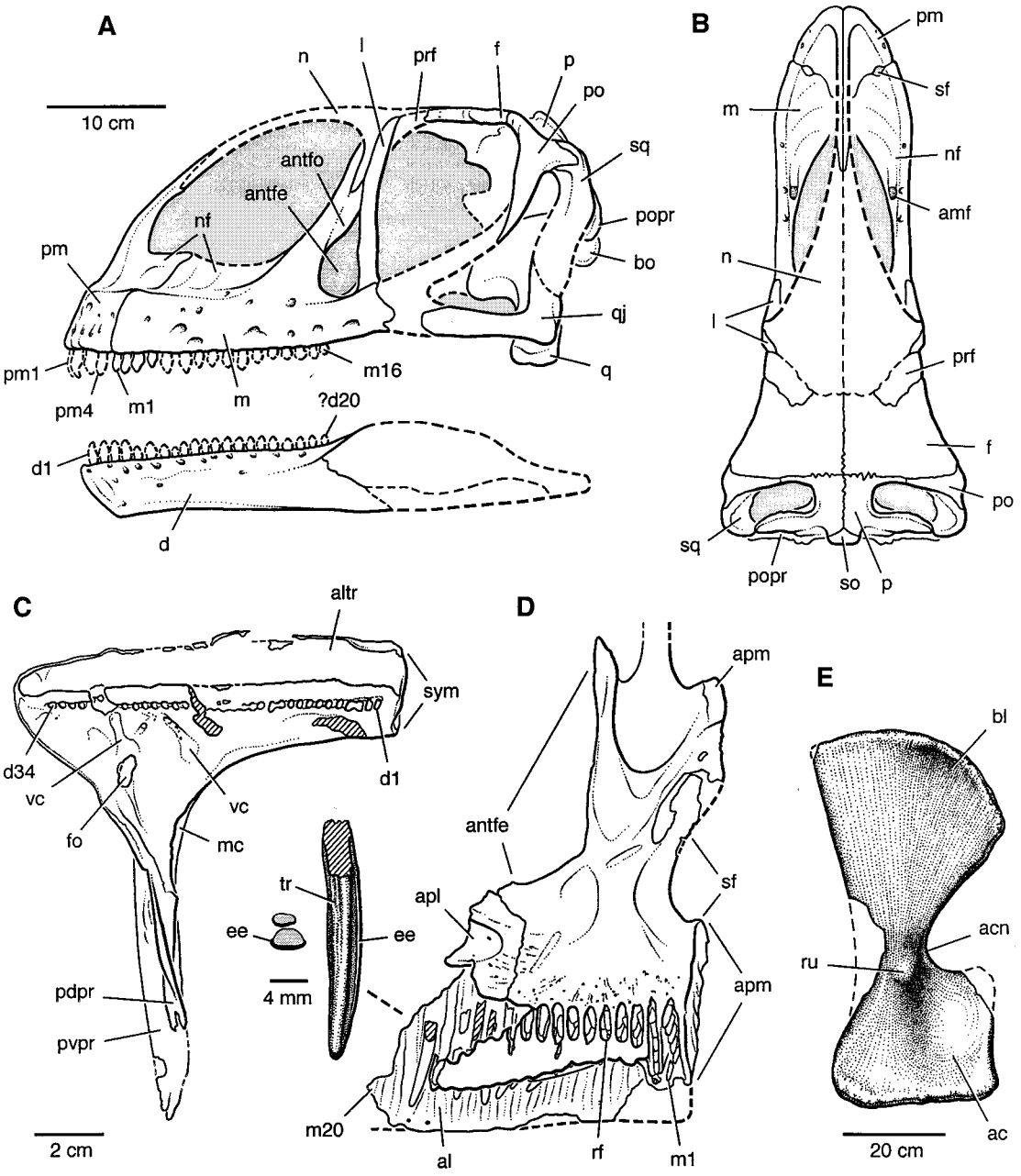


**Fig. 2.** Skull of the sauropod *Jobaria tiguidensis* (based on MNN TIG 3-5) in (**A**) left lateral and (**B**) dorsal views. Bones and teeth of the rebbachisaurid diplodocoid *Nigersaurus taqueti* (MNN GDF512), including the left dentary in dorsal view (**C**), ventral one-half of the left maxilla in posterior view, with magnified view of a maxillary crown in the seventeenth alveolus and cross sections of a pair of successive crowns in the sixth alveolus (**D**), and left scapula in medial view (**E**). In crown cross sections, enamel is shown as black and dentine as gray shading. Scale bar in (A) is also for (B); scale bar in (C) is also for (D) (except for magnified views of teeth). Abbreviations: ac, acromion; acn, acromial notch; al, alveolus; altr, alveolar trough; amf, anterior maxillary foramen; antfe, antorbital fenestra; antfo, antorbital fossa; apl, articulation for the palatine; apm, articulation for the premaxilla; bl, blade; bo, basioccipital; d, dentary; ee, enamel edge; f, frontal; fo, foramen; l, lacrimal; m, maxilla; mc, Meckel's canal; n, nasal; nf, narial fossa; p, parietal; pdpr, posterodorsal process of the dentary; pm, premaxilla; po, postorbital; popr, paroccipital process; prf, prefrontal; pvpr, posteroventral process of the dentary; q, quadrate; qj, quadratojugal; rf, replacement foramen; ru, rugosity; sf, subnarial foramen; so, supraoccipital; sq, squamosal; sym, symphysis; tr, trough for replacement crown; vc, vascular canal; and 1 to 34, tooth positions.

sandstones (*12*), and the diverse associated dinosaurian fauna includes a rare titanosaurian sauropod (*13*), the large-bodied ornithischians *Ouranosaurus* (*14*) and *Lurdosaurus* (*15*), and the spinosaurid *Suchomimus* (*16*).

In the skull, the external nares are retracted, as in more advanced diplodocoids (dicraeosaurids and diplodocids) (Fig. 2D). The shape of the snout is unique among sauropods, as best shown by the dentary (Fig. 2C). The tooth rows are oriented strictly transversely and extend lateral to the plane of the lower jaw, features unknown in any other sauropod. The symphysis for the opposing dentary is broad and circular, another unique feature. The extreme width of the symphyseal ramus most closely resembles that of a dentary attributed to *Antarctosaurus* (*17*), from rocks of Campanian age in Argentina.

In *Nigersaurus*, the teeth have gently curved slender crowns that are oval in cross section and distinguished by highly asymmetric enamel (Fig. 2D). The enamel is many times thicker on the lateral than on the medial side of the crown, a condition that has been reported previously among dinosaurs only in advanced ornithischians. There are 34 teeth in the dentary and at least 20 in the maxilla, three times as many as are present in *Diplodocus*. Replacement teeth are stacked inside the dentary and maxilla, with seven replacement teeth in the first maxillary alveolus (Fig. 2D). More than 600 teeth would have been present in the jaws of *Nigersaurus*.

Presacral vertebrae have large, sharp-rimmed pleurocoels and simple (undivided) neural spines. The broad, paddle-shaped form of the scapular blade with a broad U-shaped notch at the base of the acromial process (Fig. 2E) is similar to that in *Rayososaurus*, from Albian-Cenomanian rocks in Argentina (*9*, *18*), and *Rebbachisaurus*, a fragmentary sauropod from Cenomanian rocks in Morocco (*19*). *Nigersaurus* and the dentary referred to *Antarctosaurus* appear to be the earliest and latest known representatives, respectively, of this basal clade of diplodocoids, the Rebbachisauridae (*10*) (Fig. 4A).

The new fossils provide a framework for understanding the history of African sauropods during the Cretaceous. At least three

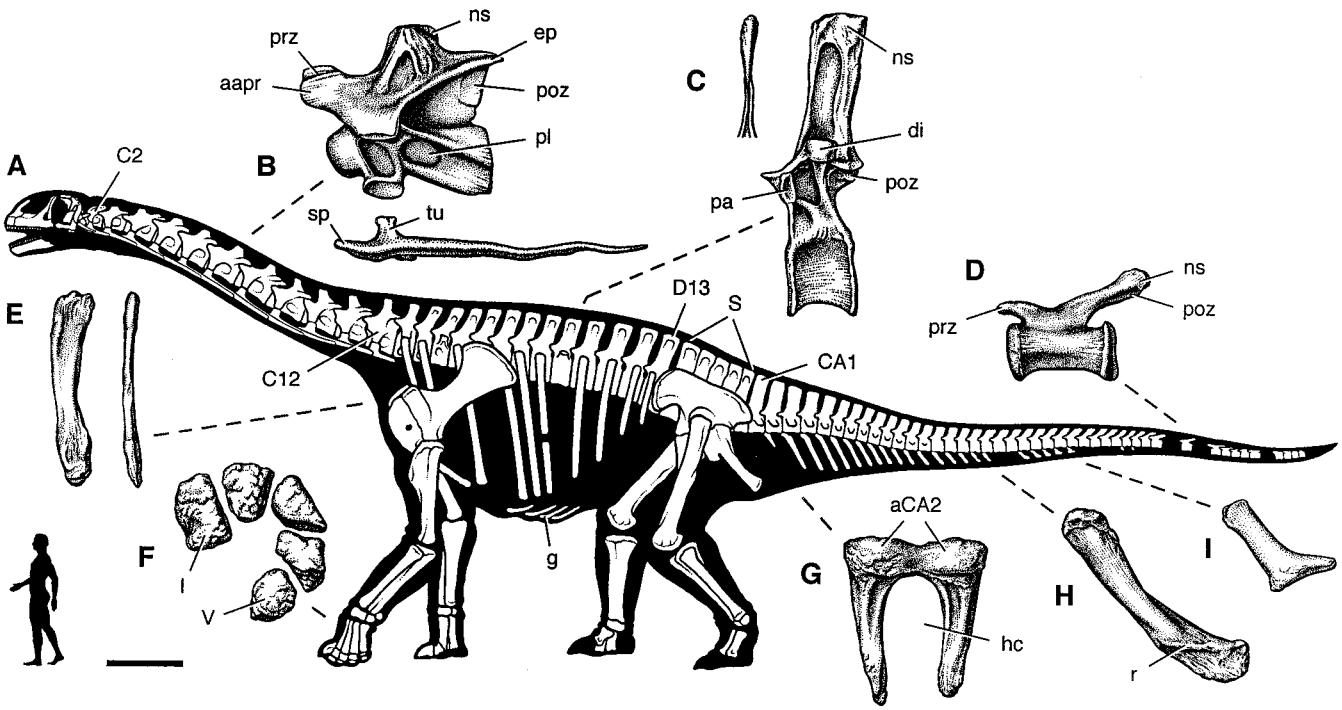


**Fig. 3.** Skeletal reconstruction of the sauropod *Jobaria tiguidensis* showing (**A**) preserved bones (about 95% of skeleton). Individual bones: (**B**) cervical 7 and associated rib in left lateral view, (**C**) dorsal 9 in left lateral view, with spine in posterior view, (**D**) caudal 35 in left lateral view, (**E**) right clavicle in anterior view (ventral end toward top) and medial view, (**F**) right metacarpus in proximal view (anterior side toward top), (**G**) chevron 1 in anterior view, (**H**) chevron 16 in left lateral view, and (**I**) chevron 24 in left lateral view. Scale bar in (A), 1 m (human silhouette, 1.68 m or 5 feet 6 inches tall; skeleton 18 m long with maximum adult length about 21 m); in (B) and (C), 20 cm; in (F), 15 cm; in (D), (E), and (G) to (I), 10 cm. Abbreviations: I, V, metacarpals I and V; aapr, accessory anterior process; aCA2, articular surface for second caudal vertebra; C, cervical; CA, caudal; D, dorsal; di, diapophysis; ep, epipophysis; g, gastralia; hc, hemal canal; ns, neural spine; pa, parapophysis; pl, pleurocoel; poz, postzygapohpyses; prz, prezygapophysis; r, ridge; S, sacral vertebrae 1 to 5 ; sp, spine; and tu, tuberculum.

lineages of sauropods survived into the Cretaceous on Africa: a primitive, broad-toothed lineage, represented by *Jobaria*, which flourished during the Neocomian but has not been recorded in younger rocks; rebbachisaurid diplodocoids, represented by *Nigersaurus*, which now are recorded from the Aptian-Albian through the Cenomanian, although unknown in post-Cenomanian rocks; and basal titanosaurs, such as *Malawisaurus* (*20*), which were present during the Early Cretaceous but appear to have been relatively rare at least through the Cenomanian (*21*).

A slow rate of evolutionary change seems to characterize the lineage that gave rise to *Jobaria*. To more adequately gauge the quality of the dinosaurian fossil record and what that record implies about rates of skeletal change among dinosaurs generally, we plotted (i) the order of the first occurrence of 70 nonavian dinosaurian taxa (age rank) (*22*) against their predicted order of divergence based on phylogenetic analysis (clade rank) (*23*) (Fig. 4B) and (ii) the number of skeletal changes per node (total synapomorphies) in dinosaurian phylogeny (*24*) against the minimum elapsed time during which those changes must have arisen (minimum missing ancestral lineage) (*25*) (Fig. 4C).

The dinosaurian fossil record, like that of basal synapsids and several nonvertebrate groups (*26*–*28*), shows significant positive correlation between age and clade rank (Fig. 4B). This is apparent in sauropods, despite the presence of missing ancestral lineages of significant duration (*29*) (Fig. 4A). Stratigraphic data thus carry some phylogenetic signal among dinosaurs (*1*, *30*).

Skeletal change between these same taxa, in contrast, shows little discernible correlation with estimates of elapsed time (Fig. 4C). The number of synapomorphies between nodes in higher level dinosaurian phylogeny, unlike that for basal nodes within synapsids (*28*), shows little or no correlation with estimates of the duration of missing ancestral lineages. Sauropods, for example, exhibit slow rates of skeletal change in the Early and Middle Jurassic, when the relevant missing ancestral lineages are relatively long (*31*) (Fig. 4A). Nor can this result be understood as particular to the phylogenetic survey used in the correlations (*4*); a similar lack of correlation between skeletal change and elapsed time exists in alternative phylogenetic analyses (*32*).

These data provide the first quantitative assessment of rates of skeletal change among dinosaurs, the best documented terrestrial radiation of the Mesozoic. Some lineages, such as that leading to *Jobaria*, remained relatively static for tens of millions of years, whereas others changed rapidly. Considerable variation in the rate of skeletal change appears to have been the norm in dinosaur evolution.

### References and Notes

1. P. C. Sereno, *Annu. Rev. Earth Planet. Sci.* **1997**, 435 (1997).
2. L. Salgado and J. F. Bonaparte, *Ameghiniana* **28**, 333 (1991); P. C. Sereno *et al.*, *Science* **272**, 986 (1996); R. A. Coria and L. Salgado, *Nature* **377**, 224 (1995); *J. Vertebr. Paleontol.* **16**, 445 (1996); S. L. Jain and S. Bandyopadhyay, *J. Vertebr. Paleontol.* **17**, 114 (1997); S. D. Sampson *et al.*, *Science* **280**, 1048 (1998). See also (*20*).
3. P. C. Sereno, J. A. Wilson, H. C. E. Larsson, D. B. Dutheil, H.-D. Sues, *Science* **266**, 267 (1994).
4. P. C. Sereno, *Science* **284**, 2137 (1999).
5. Fragmentary sauropod remains from the Tiourarén Formation were initially described as a new species, *Rebbachisaurus tamesnensis* [A. F. de Lapparent, *Mém. Soc. Géol. France* **88A**, 1 (1960)]. Type material, however, was not designated, and no diagnostic features were mentioned (*3*). Lapparent considered the Tiourarén sauropod to be a camarasaurid; elsewhere it has been referred to the Diplodocidae [J. S. McIntosh, in *The Dinosauria* (Univ. of California Press, Berkeley, CA, 1990), pp. 345–401]. **Etymology**: *Jobar*, Jobar (Tamacheck); *ia*, pertaining to (Greek); *tiguidi*, Tiguidi (Tamacheck); *ensis*, from (Latin). Named after the mythical creature "Jobar," to whom local Touregs had attributed the exposed bones, and after the Falaise de Tiguidi, a cliff near the base of which lie the horizons yielding all of its remains. **Holotype**: Partial articulated skeleton including the axis, forelimbs and hind limbs, pubes, and most of the tail, from the locality Tamérat, cataloged in the collections of the Musée National du Niger (MNN TIG3),

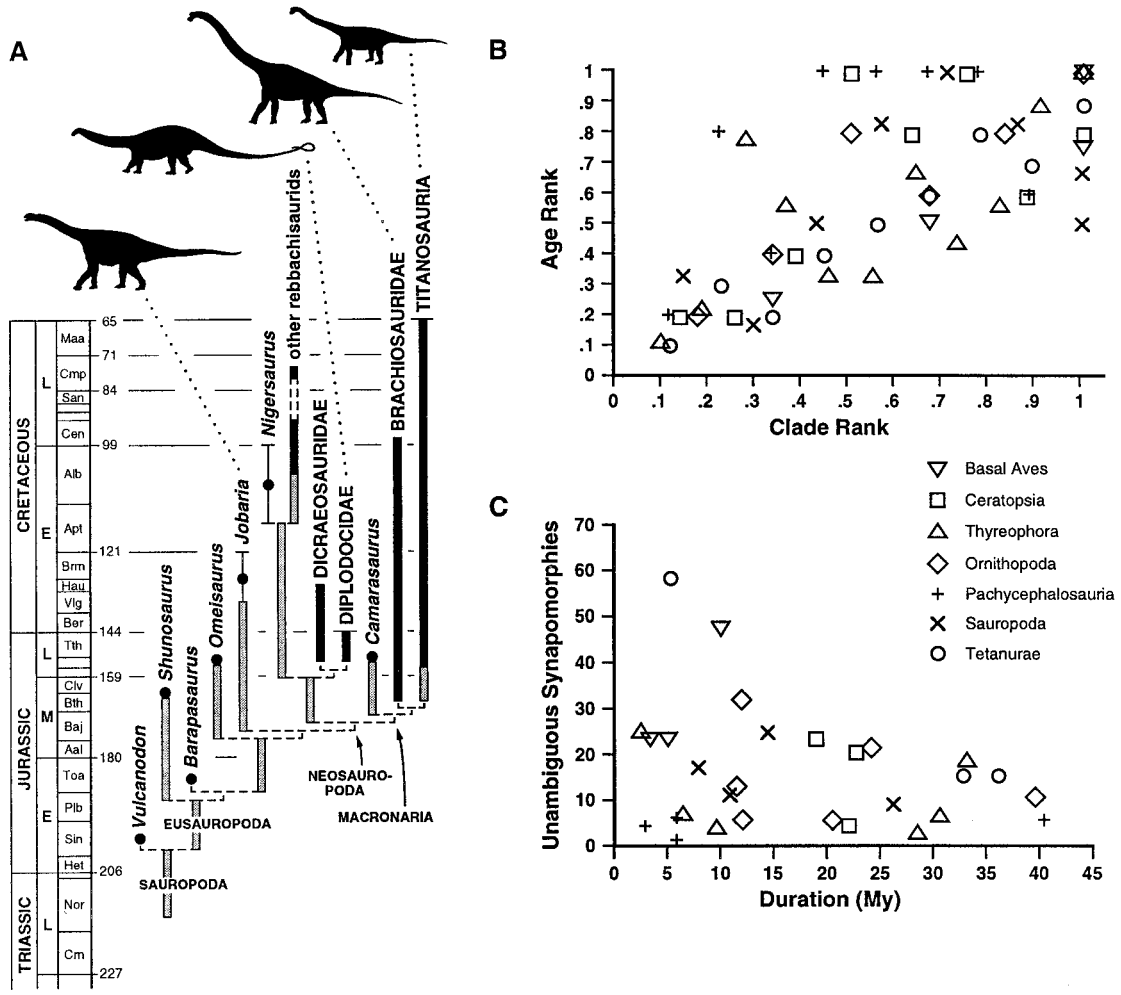


**Fig. 4.** (**A**) Calibrated phylogeny of sauropods (*9*, *10*) showing the phylogenetic position of *Jobaria tiguidensis* and *Nigersaurus taqueti*. The phylogenetic position of *Jobaria* is stable in trees two steps longer than the minimum-length tree. Solid dots and bars indicate recorded occurrence, shaded bars estimate missing range, and error bars indicate age uncertainty. Temporal values for stage boundaries are based on a recent time scale (*33*). Numbers indicate age in millions of years ago. (**B**) Plot of age rank versus clade rank (scaled from 0 to 1) for 72 genera or suprageneric taxa of dinosaurs based on recent phylogenetic analyses (*4*, *9*) and temporal estimates calculated from a recent time scale (*33*). Spearman rank correlation (corrected for ties) is positive and significant ($S = 0.709$, $P < 0.0001$). (**C**) Plot of unambiguous synapomorphies versus the minimum duration of missing ancestral lineage [millions of years (My)] for the same set of taxa. Spearman rank correlation (corrected for ties) is negative and not significant ($S = -0.151$, $P = 0.4256$). Except for two outlier nodes (Paraves and Ornithothoraces) that show more than 45 skeletal changes over less than 10 million years, the majority of nodes in dinosaurian phylogeny show 30 or fewer changes accumulating over durations ranging from 3 to 40 million years. Cladograms, age and clade rank data, synapomorphy counts, and estimates of the minimum durations for missing ancestral lineages are available at www.sciencemag.org/feature/data/1045224.shl.

Niamey, Republic of Niger. **Referred material**: Several partial skeletons and isolated bones from Fako, Tawachi, and other localities near the base of the Falaise de Tiguidi (Fig. 1A). Specimens include a partial skull and skeletons of adult individuals (MNN TIG4 and -5), a relatively complete subadult skeleton (MNN TIG6), and an isolated subadult braincase (MNN TIG7). **Diagnosis**: Eusauropod characterized by cervical prezygapophyses with an accessory anterior process (Fig. 3B, aapr), cervical neural arches with a deep fossa between centropostzygapophyseal and intrapostzygapophyseal laminae, dorsal prezygapophyses with a broad pendant flange, dorsal neural arches with fossa between the parapophyses and diapophyses (Fig. 3C), anterior caudal neural spines with a circular fossa at the base of the prespinal lamina, cervical ribs 3 to 6 with an accessory anterior process, U-shaped first chevron (Fig. 3G), and mid-caudal chevrons with a rugose ridge across the distal end of blade (Fig. 3H, r).


6. R. T. J. Moody and P. J. C. Sutcliffe, *Cretaceous. Res.* **12**, 137 (1991). Principal exposures of the Tiourarén Formation lie in an arc north of the Falaise de Tiguidi, which is formed by the resistant basal sandstone of the Tegama Group (Fig. 1, B and C). Nearly all fossils were found 20 to 30 m below the contact with the Tegama Group in sedimentary rocks consisting primarily of clay-rich overbank deposits with developed paleosols and rare fluvial channels. The Fako locality comprises two bone-bearing units. The lower one is a 50-cm-thick crevasse splay deposit that rapidly covered scavenged carcasses of *Jobaria*, including an adult individual with an estimated body length of 18 m (Fig. 3A) resting on a subadult individual about 75% its size.
7. Despite relatively flat zygapophyseal articular surfaces, living long-necked herbivores (for example, *Camelus domesticus*, the dromedary camel) routinely engage in extreme neck postures. Sauropod necks, in general, may have been more flexible than inferred from computer modeling [K. A. Stevens and J. M. Parrish, *Science* **284**, 798 (1999)].
8. O. C. Marsh, *U.S. Geol. Surv. 16th Annu. Rep.* **1894–1895**, 133 (1896); B. J. Filla and P. D. Redman, *Wyoming Geol. Assoc. Guideb.* **1994**, 159 (1994).
9. J. A. Wilson and P. C. Sereno, *J. Vertebr. Paleontol.* **18**, 1 (1998).
10. J. A. Wilson, thesis, University of Chicago (1999).
11. Originally described as a dicraeosaurid and allied with titanosaurs (*14*), the Gadoufaoua sauropod is better understood as a rebbachisaurid diplodocoid. **Etymology**: *Niger*, for the Republique du Niger; *sauros*, reptile (Greek); *taqueti*, after Philippe Taquet. Named after the country of origin and after French paleontologist Philippe Taquet, whose expeditions (1965–72) initiated large-scale paleontological exploration in Niger. **Holotype**: Partial articulated skeleton from the locality "niveau des Innocents" in the Gadoufaoua region (16°, 27′ latitude, 9°, 8′ longitude) that includes a partial skull (Fig. 2, C and D), neck, scapula, forelimbs, and hind limbs, cataloged in the collections of the Musée National du Niger (MNN GAD512), Niamey, Republic of Niger. **Referred material**: Several partial skeletons and isolated bones from other localities in Gadoufaoua (Fig. 2E). **Diagnosis**: Rebbachisaurid characterized by elongate frontal (much narrower than long) with a marked cerebral fossa on the frontal, transversely oriented upper and lower tooth rows, extension of the tooth rows lateral to the plane of the principal ramus of the lower jaw, tooth crowns with prominent medial and lateral marginal ridges, dorsal vertebrae with paired pneumatic spaces at the base of the neural spines, and a prominent rugosity on the medial aspect of the base of the scapular blade (Fig. 2E, ru).
12. The Tegama Group is composed of terrestrial rocks of mid to Late Cretaceous age that are divided into three formations [H. Faure, *Mém. B.R.G.M.* **47**, 1 (1966); J. Greigert and R. Pougnet, *Mém. B.R.G.M.* **48**, 1 (1967)] (Fig. 1D). In the region called Gadoufaoua southeast of the Aïr Mountains (Fig. 1A), the Tegama Group was divided into eight GAD levels ["GAD" is an abbreviation for Gadoufaoua; E. Molinas, *Rapp. C.E.A. Marseille* **1965**, 1 (1965)]. GAD 5 corresponds with the upper part of the Elrhaz Formation and the lower part of the Echkar Formation, which yielded all of the sauropod remains described here from the Tegama Group.
13. Diagnostic titanosaur remains include a tall, transversely narrow astragalus (*10*) and procoelous caudal vertebrae with spongy bone and a neural arch shifted to the anterior end of the centrum.
14. P. Taquet, *Cah. Paléontol.* **1976**, 1 (1976).
15. _____ and D. A. Russell, *Ann. Paléontol.* **85**, 85 (1999).
16. P. C. Sereno *et al.*, *Science* **282**, 1298 (1998).
17. F. von Huene, *An. Mus. La Plata Ser. 2* **3**, 1 (1929).

18. J. O. Calvo and L. Salgado, *Gaia* **11**, 13 (1995).
19. R. Lavocat, *C. R. 19th Int. Geol. Congr.* **3**, 65 (1954).
20. L. L. Jacobs, D. A. Winkler, W. R. Downs, E. M. Gomani, *Palaeontology* **36**, 523 (1993).
21. E. Stromer, *Abh. Bayer. Akad. Wiss. Math. Naturwiss. Abt.* **22**, 1 (1934).
22. Age rank was established with the midpoint of the first stage (or longer temporal unit) in which the taxon has been recorded. Midpoint values were calculated from a recent time scale (*33*). Age rank was scaled from 0 to 1.
23. Clade rank (*26*) was established with recent phylogenetic analyses for Dinosauria (*4*, *9*) with a few terminal taxa collapsed or omitted to achieve single most parsimonious, fully asymmetric cladograms. Clade rank was scaled from 0 to 1.
24. Only unambiguous character-state changes are plotted. If there was no missing ancestral lineage between two or more nodes on the tree (that is, 0 duration), synapomorphies were added to those associated with the next positive duration [method 2 of (*28*)].
25. The minimum duration for missing ancestral lineages ["ghost taxa"; M. A. Norell, *Am. J. Sci.* **293A**, 407 (1993)] was calculated by subtracting the midpoints of the first occurrence dates at successive nodes.
26. J. A. Gauthier, A. J. Kluge, T. Rowe, *Cladistics* **4**, 105 (1988); M. A. Norell and M. J. Novacek, *Cladistics* **8**, 319 (1992).
27. A. B. Smith, B. Lafay, R. Christen, *Philos. Trans. R. Soc. London Ser. B Biol. Sci.* **338**, 365 (1992).
28. C. A. Sidor and J. A. Hopson, *Paleobiology* **24**, 254 (1998); P. J. Wagner and C. A. Sidor, *Syst. Biol.*, in press.
29. The greatest missing lineages in higher level sauropod phylogeny occur at the base of sauropod phylogeny, but most of the terminal taxa (except *Shunosaurus*) still appear successively in time. Spearman rank correlation (corrected for ties) is positive ($S = 0.603$) and significant ($P = 0.0035$).
30. D. L. Fox, D. C. Fisher, L. R. Leighton, *Science* **284**, 1816 (1999).
31. In higher level sauropod phylogeny, missing temporal lineages are shortest or nonexistent at the base of the neosauropod radiation, where a greater amount of skeletal change is known to have occurred. Within Sauropoda, skeletal change is not positively correlated with the duration of missing lineages or significant [Spearman rank correlation (corrected for ties) is negative ($S = -1.00$, $P = 0.1573$)].
32. An alternative data matrix for tetanuran theropods [T. R. Holtz Jr., *J. Paleontol.* **68**, 1100 (1994)] was sampled with some terminal taxa collapsed or omitted to achieve a single most parsimonious cladogram. No iteration could produce a positive or significant correlation between the number of unambiguous synapomorphies and estimated elapsed time.
33. F. M. Gradstein *et al.*, *Soc. Econ. Paleontol. Mineral. Spec. Publ.* **54**, 95 (1995).
34. A. G. Smith, D. G. Smith, B. M. Funnell, *Atlas of Mesozoic and Cenozoic Coastlines* (Cambridge Univ. Press, Cambridge, 1994).
35. Y. Zhang, *The Middle Jurassic Dinosaur Fauna from Dashanpu, Zigong, Sichuan* (Sichuan Publishing House of Science Technology, Chengdu, China, 1988).
36. J. S. McIntosh, C. A. Miles, K. C. Cloward, J. R. Parker, *Bull. Gunma Mus. Nat. Hist.* **1**, 1 (1996).
37. C. W. Gilmore, *Mem. Carnegie Mus.* **10**, 347 (1925).
38. Supported by the David and Lucile Packard Foundation, the National Geographic Society, the Pritzker Foundation, and the Women's Board of the University of Chicago. We thank C. Abraczinskas for drawing original specimens and executing the final drafts of all other figures; Q. Cao, D. Blackburn, J. Conrad, E. Dong, J. Komar, E. Love, C. Noto, and volunteer staff for fossil preparation and casting; and J. Conrad, J. Hopson, and F. Lando for reviewing an earlier draft of this report. We acknowledge the assistance of I. Kouada and B. Gado of the Ministère de L'Enseignement Supérieur de la Recherche et de la Technologie and Institut de Recherches en Sciences Humaine, respectively (Niger). For permission to conduct field work, we are indebted to the Republique du Niger.

8 September 1999; accepted 19 October 1999

# Prolonged Activation of Mitochondrial Conductances During Synaptic Transmission

**Elizabeth A. Jonas,[1] JoAnn Buchanan,[2] Leonard K. Kaczmarek[1]***

**Although ion channels have been detected in mitochondria, scientists have not been able to record ion transport in mitochondria of intact cells. A variation of the patch clamp technique was used to record ion channel activity from intracellular organelles in the presynaptic terminal of the squid. Electron microscopy indicated that mitochondria are numerous in this terminal and are the only organelles compatible with the tips of the pipettes. Before synaptic stimulation, channel activity was infrequent and its conductance was small, although large conductances (~0.5 to 2.5 nanosiemens) could be detected occasionally. During a train of action potentials, the conductance of the mitochondrial membrane increased up to 60-fold. The conductance increased after a delay of several hundred milliseconds and continued to increase after stimulation had stopped. Recovery occurred over tens of seconds.**

Intracellular calcium stores are important in the function of excitable cells (*1, 2*). For example, mitochondrial calcium uptake followed by rapid re-release from the mitochondrial matrix shapes the time course of calcium transients during synaptic activity and prolongs the elevated levels of intracellular calcium (also called "residual calcium") that underlie post-tetanic potentiation (PTP) (*3*).

Mitochondria take up calcium in response to localized elevations in calcium (*4*). Extrusion of protons from the inner mitochondrial matrix produces a large (−160 to −200 mV) voltage gradient across the inner mitochondrial membrane (*5*). Calcium can therefore flow readily along its electrochemical gradient into the mitochondrial matrix (*6*). At rest, the level of free calcium in the matrix is similar to the cytosolic level, but total mitochondrial calcium can increase markedly during depolarization (*2, 7*). High levels of intramitochondrial calcium interact with matrix enzymes and then exit rapidly, which allows the mitochondria to regain their pre-stimulation levels within 5 min of a cytosolic load (*2, 8*).

Studies on isolated mitochondria or artificial lipid bilayer preparations have revealed several types of ion channels on both inner and outer mitochondrial membranes (*9–13*). However, no technique was available to record ion channel activity from intracellular membranes in intact cells. We have recently described the use of such a technique (*14*), and we have applied it here to the giant presynaptic terminal of the squid.

With electron microscopy, we determined that the dominant structures in the central region of the presynaptic terminal are mitochondria and neurofilaments (Fig. 1) (*15*). Clusters of synaptic vesicles occur at active zones and, occasionally, in more central regions. Vesicle size (50 nm) is too small, however, to allow seal formation across the tips of the pipettes. Thin strips of membranes, possibly from endoplasmic reticula, could also be detected sometimes but accounted for less than ~2% of the internal membranes. Thus the mitochondria (Fig. 1), whose cross-sectional diameters range from ~300 to 1200 nm [mean = 575 ± 181 (SD) nm, $n = 15$] are the only internal organelles that are compatible with seal formation by the patch pipettes, which have tip diameters of ~180 to 200 nm (*16*).

Seals (0.5 to 6.0 gigohm) were obtained in 94 experiments using the technique in (*17*); 71 of the 94 seals were greater than 1.5 gigohm. The successful recordings represented approximately 40% of attempts. When a fluorescent lipophilic dye was included in the patch pipette, a fluorescent signal could be detected only after a high-resistance seal was obtained ($n = 7$). The fluorescent signals in all the dye experiments were located within the large terminal finger of the presynaptic terminal (*18*).

After formation of a gigohm seal, the potential of the patch was set between −100 and +100 mV to record the spontaneous and voltage-dependent activity in the membranes. We observed spontaneous channel activity in 50% of the seals ($n = 47$ out of 94) and the amplitude of such activity was usually low. In many

[1]Department of Pharmacology, Yale University School of Medicine, New Haven, CT 06520, USA. [2]Department of Molecular and Cellular Physiology, Stanford University Medical Center, Stanford, CA 94305, USA.

*To whom correspondence should be addressed. E-mail: leonard.kaczmarek@yale.edu